



# CONSTRAINED EVOLUTION: CONCEPTS AND NEW RESULTS

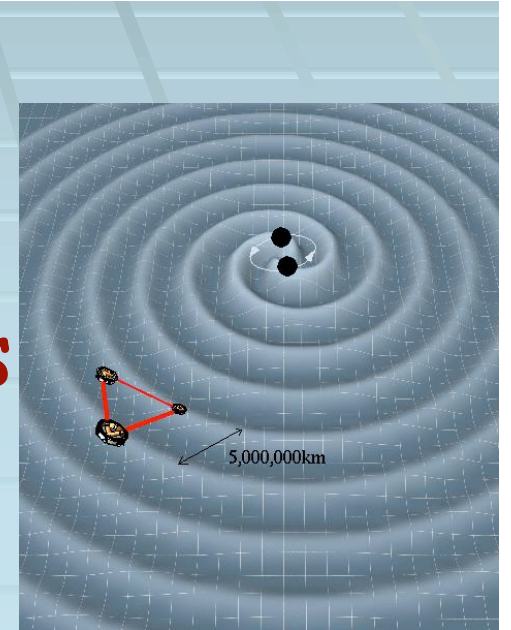
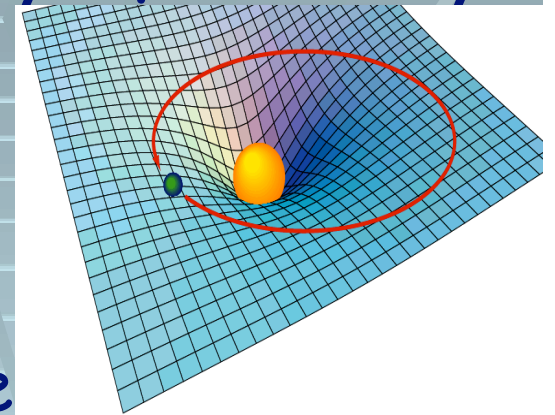
Richard Matzner

University of Texas at Austin

Aspen Center for Physics  
February 2004

# General Relativity

- General Relativity is the Theory of Gravity
- GR describes Gravity as curvature
- GR "is" Newtonian Theory plus waves



# Newtonian Gravity

- (Poisson:)  $\nabla^2 \phi = \phi_{,i}^i = 4\pi \rho$  *source*

## Waves: like E&M

- (divergence:)  $E^i_{,i} = \text{source}$

- (wave equation)  $\frac{\partial A_i}{\partial t} = E_i + \dots$

$$\begin{aligned} \frac{\partial E_i}{\partial t} &= [\nabla \cdot (\nabla \times A)]_i \\ &= \nabla^2 A_i + \dots \end{aligned}$$

# General Relativity

- (Poisson)  $\square^2 \square = \frac{1}{8} [\tilde{R} \square + \frac{2}{3} \tilde{K}^2 \square^{\bar{p}}$   
 $+ \square^{\bar{p}^7} (\tilde{K}_a^b - \frac{1}{3} \square_a^b \tilde{K}) (\tilde{K}_b^a - \frac{1}{3} \square_b^a \tilde{K})] + src$

- (Divergence)  $\square_i (K_j^i - \frac{1}{3} \square_j K^b_b) = src'_j$   
*( $K_{ij}$  is the analog of  $E_i$ )*

- (Wave Equation):  $\frac{\partial}{\partial t} g_{ij} = -2K_{ij}$   
 $\frac{\partial}{\partial t} K_{ij} = R_{ij} + K_i^c K_{jc} + K_{ij} K^a_a$

(special coordinates)

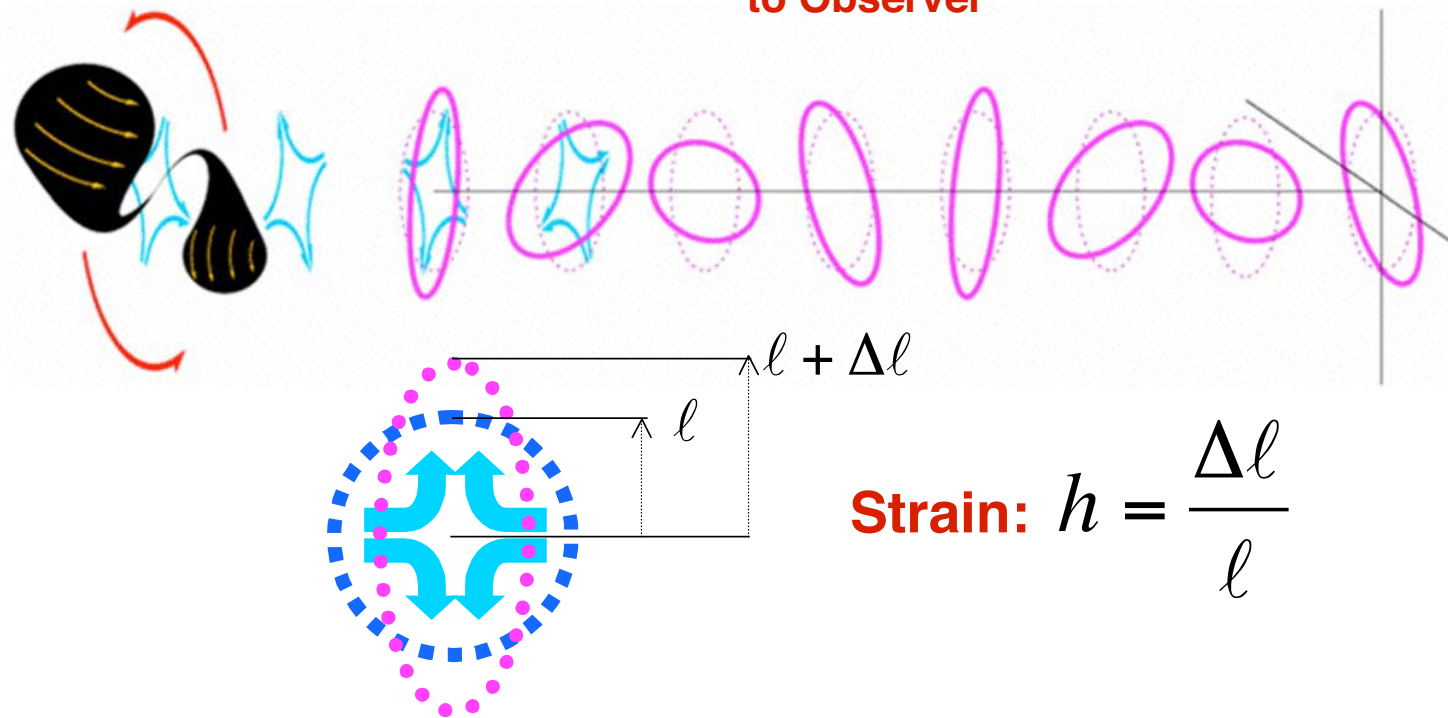


# Gravitational Radiation and Detectors: Gravitational Radiation

**Source: Bulk Motion  
Produces Changing Tidal Field**

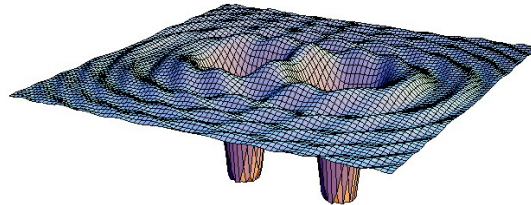
**Oscillating Tidal Field  
Propagates (Unobstructed)  
to Observer**

**Observer Detects  
Distortion Strain**



**Strain:**  $h = \frac{\Delta l}{l}$

## Binary black holes



*From the GW detection point of view:* the most promising source

*From the theoretical point of view:*

- Binary BH = the two body problem in General Relativity
- Extreme GR  $\implies$  probes the limit of GR (as weak field limit of string theory)

*From the astrophysical point of view:*

- Rate of binary black hole coalescence  $\implies$  massive star evolution
- Inspiral GW signal  $\implies$  precise measure of Hubble constant  $H_0$
- GW observations of supermassive BH at high  $z$   $\implies$  large structure formation

# GR "is" Newtonian Gravity plus waves

3-metric is analog of  $A_i$

$$g_{ij} = \square^4 \tilde{g}_{ij}$$

TRIAL METRIC

ANALOG OF NEWTONIAN  $\square$

# GR "is" Newtonian Gravity plus waves

$\square$  modifies your "trial"  $\tilde{g}_{ij}$ .

Choose well, and  $\square \sim 1$ .

$$g_{ij} = \square^{\#} \tilde{g}_{ij}$$

← TRIAL METRIC

$\square \sim 1$ : physically motivated guess close to actual data



# KERR-SCHILD FORM

Schwarzschild:  $M/r$

- Metric  $g_{ab} = \text{flat space} + \text{pole}$

• **EXACT BLACK HOLE SOLUTION!**

--Kerr, or Schwarzschild--

# KERR-SCHILD MULTI-BH DATA SETTING

## Approximate ( $g_{ab}$ )

- Metric  $\tilde{g}_{ab} = \text{flat space} + \text{pole}_1 + \text{pole}_2$   
     $\swarrow M_1/r_1$        $\nwarrow M_2/r_2$

### • APPROXIMATE 2-BLACK HOLE SOLUTION-

--Kerr, or Schwarzschild

--arbitrary mass, spin, location, momentum

# KERR-SCHILD MULTI-BH DATA SETTING

Approximate ( $g_{ab}$ )

$$g_{ab} = \square^A \tilde{g}_{ab}; \quad \text{find } \square \parallel 1$$

-differences less than 1%

## GOOD WAY TO SET DATA!

- $K_{ab}$  changes are small also

# Getting Started: INITIAL DATA

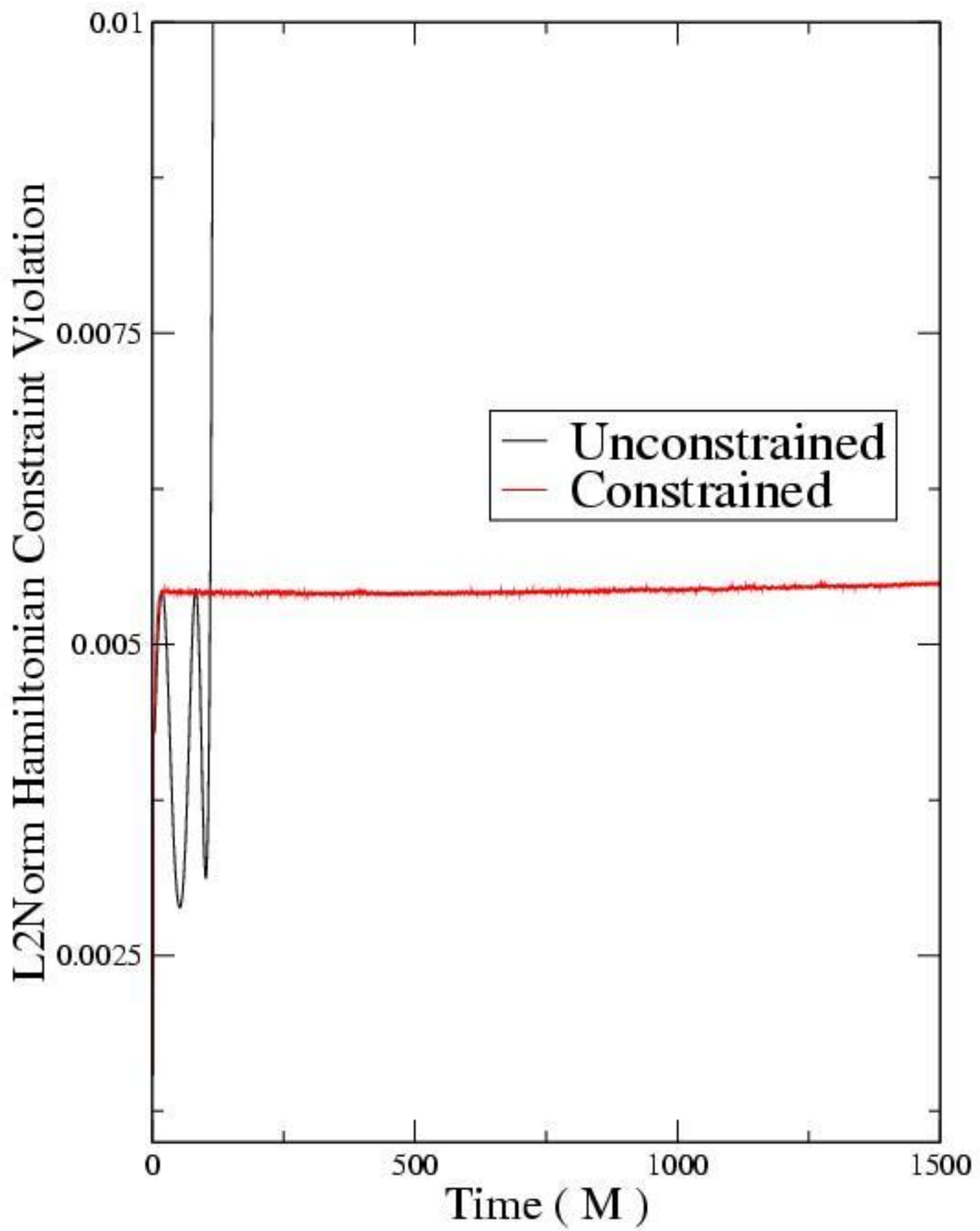
- INITIAL DATA (CONSTRAINT EQUATIONS)
- Solve them first-
- Then evolution ("wave") equation preserves the constraints *analytically*.

# EVOLUTION in Full GR (e.g. vacuum Binary B H)

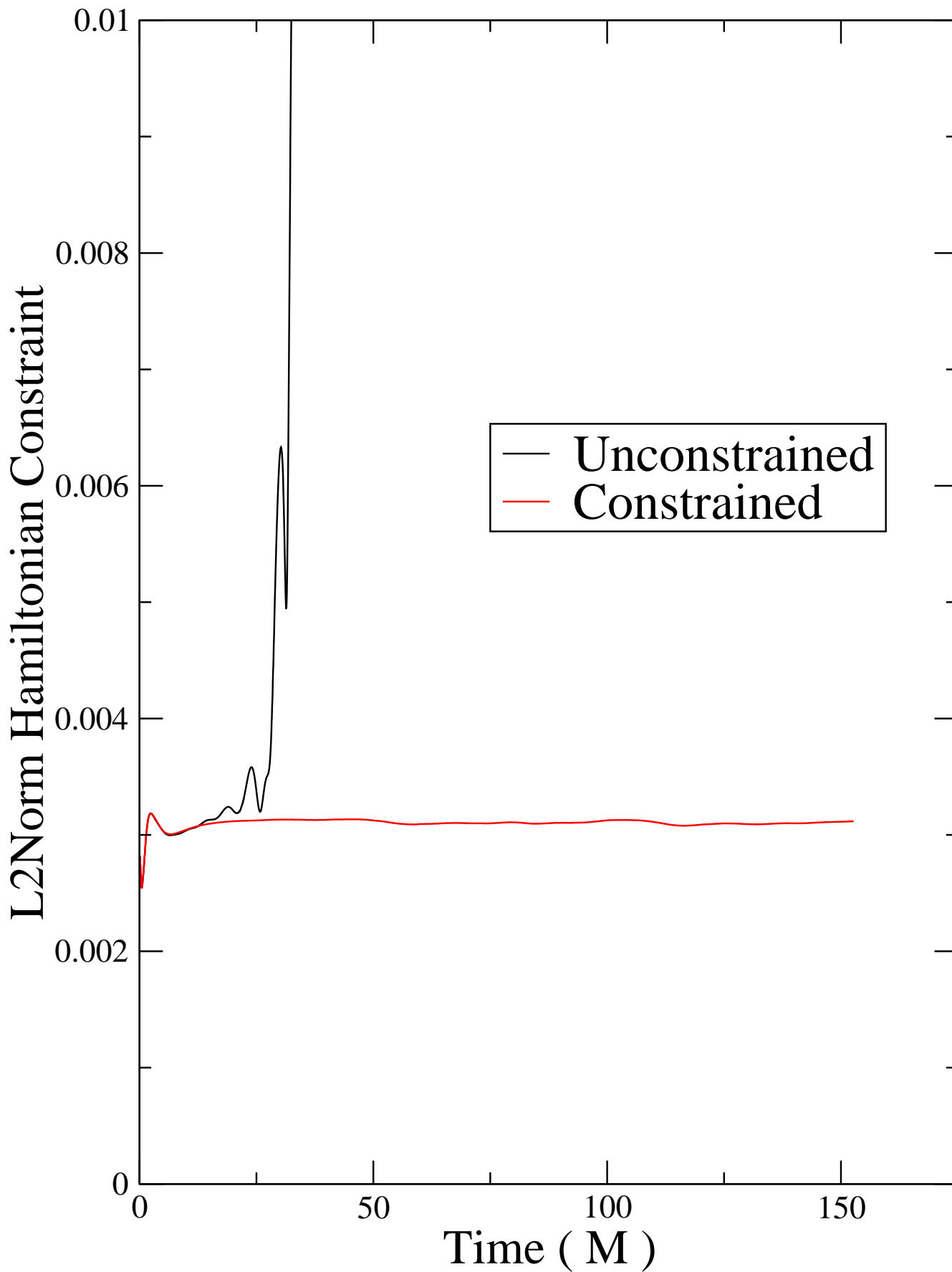
- Solve initial data problem
- Evolve time equations one step,  
get new  $g_{ab}, K_{ab}$ .
- Use this new  $g_{ab}$  as  $\tilde{g}_{ab}$  in a new initial data solve:  
 $\delta = 1 + \epsilon \quad |\epsilon| \ll \ll 1; \quad \text{change in } K_{ab} \ll \ll \ll 1.$   
----this gives definitive  $g_{ab} K_{ab}$
- REPEAT

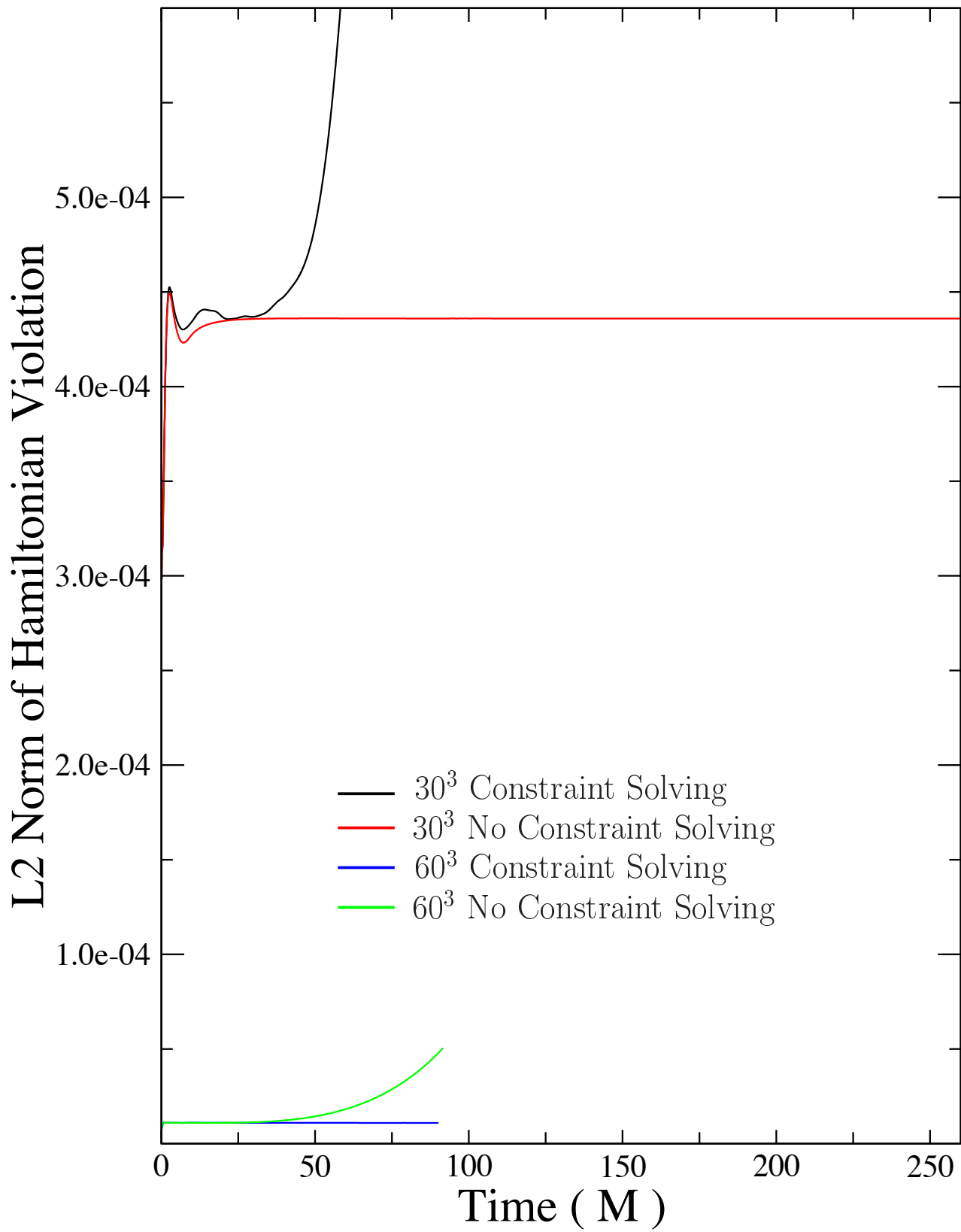
("linearization")

# 1-D Constrained Evolution

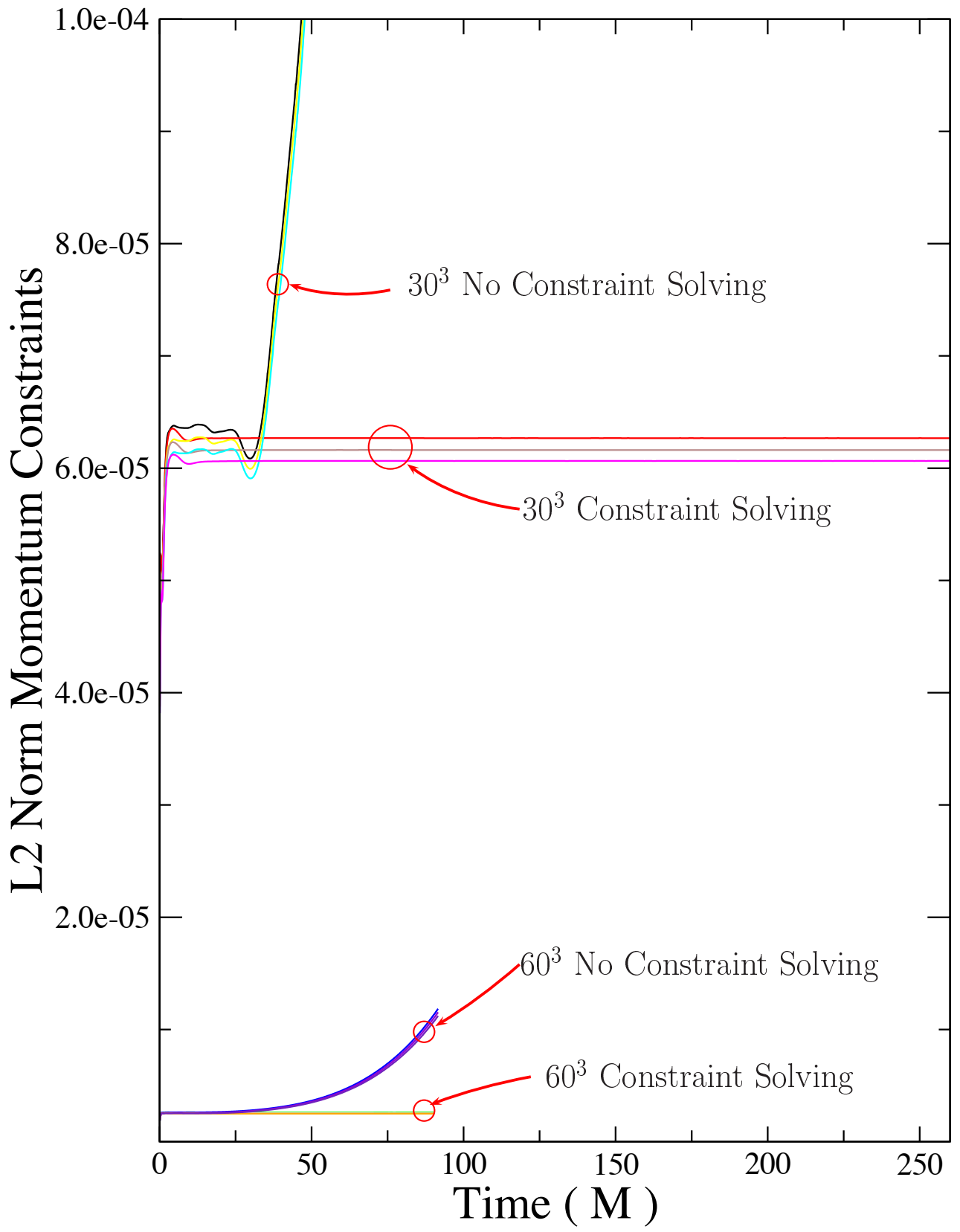


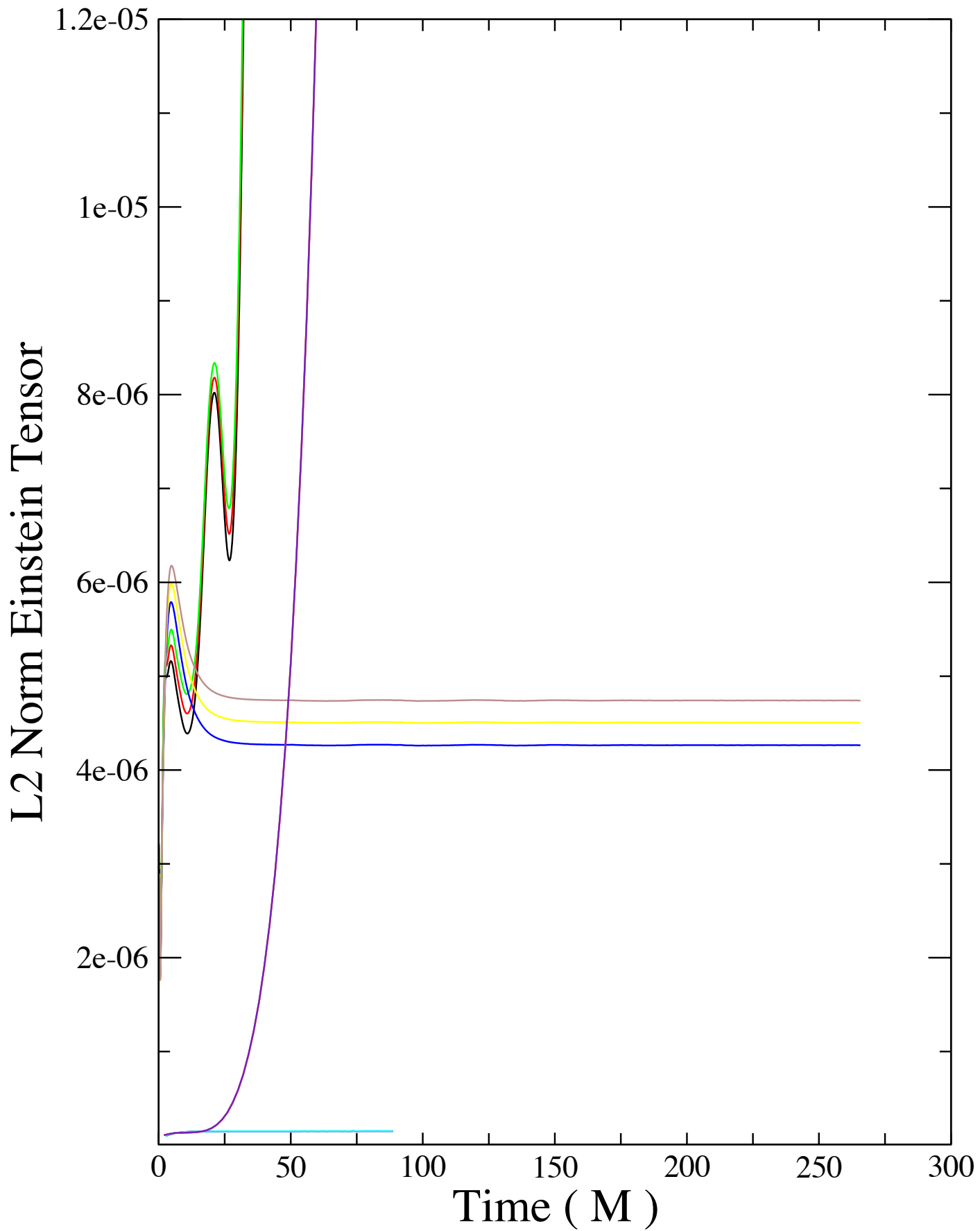
# 3-D Constrained Evolution

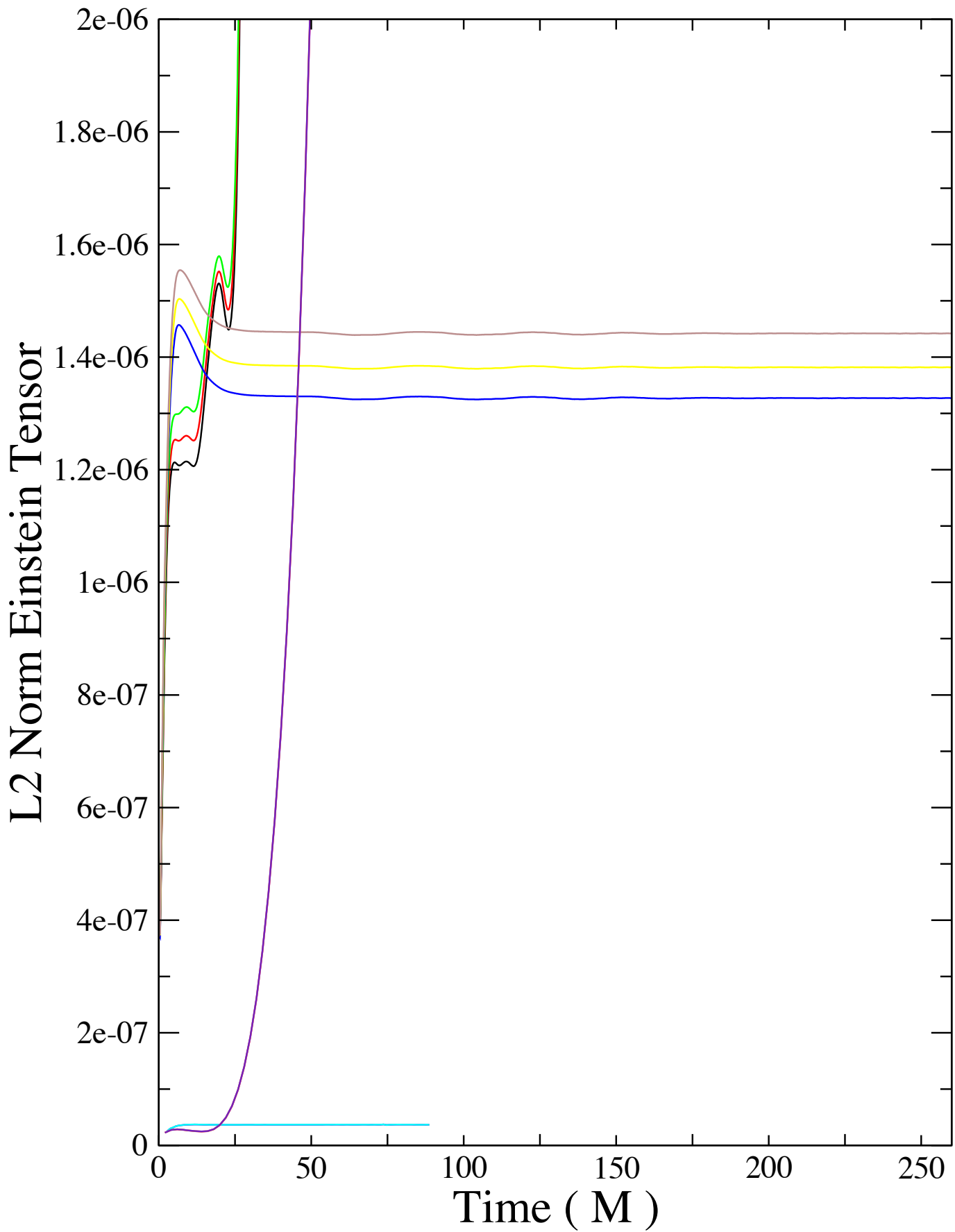


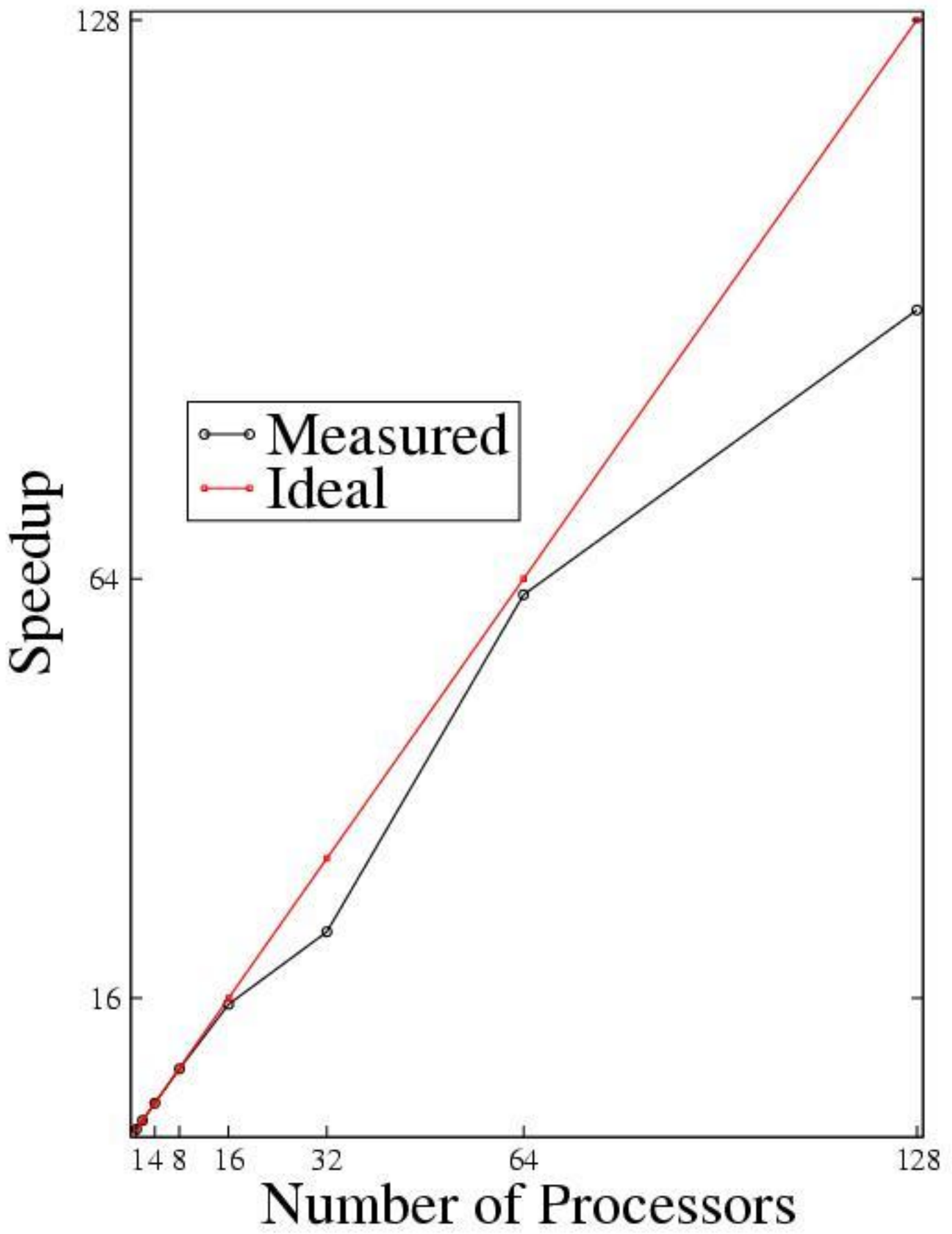












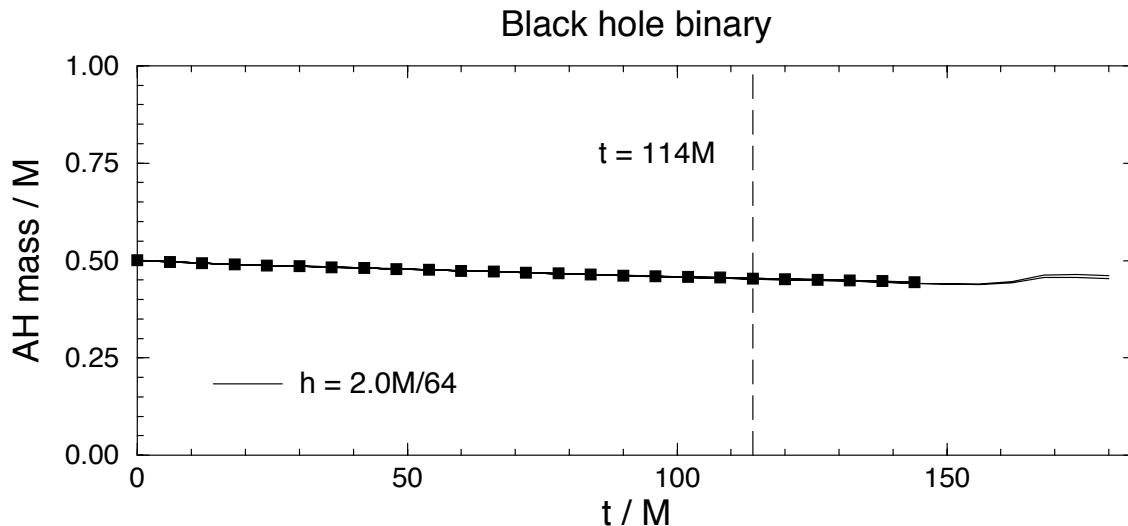


Figure 1: Evolution of the AH mass for the black hole binary with  $\rho_0 = 3.0M$ . The evolution lasts longer than one orbital period of  $114M$  defined by the initial data. The squares mark a run with 7 nested levels with coarsest resolution  $2M$  and finest resolution  $h = 0.03125M$ , and with the spherical outer boundary at about  $48M$ , which crashes around  $145M$ . Also plotted are results from seven control runs with the outer boundary at  $24M$  and  $96M$ , with a cubical outer boundary, and with the AH extracted on a coarser grid to check its convergence. (Bruegmann, Tichy, Jansen, gr-qc/0312112).

## Black hole binary, apparent horizon

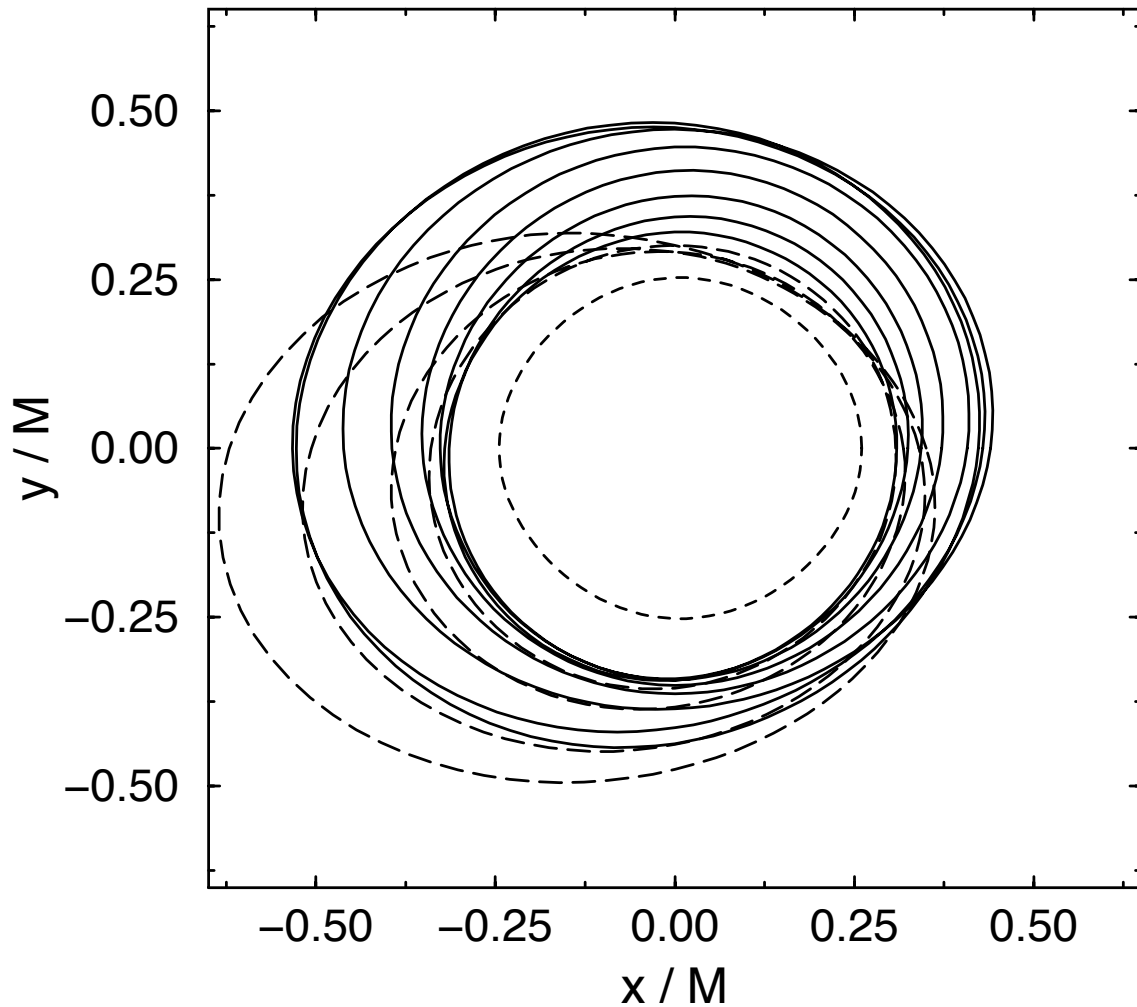


Figure 2: The coordinate location of the AH around one of the black holes in the  $x$ - $y$ -plane is shown every  $12M$  for a typical run. The AH starts as the smallest circle (dashed) in the center, quickly moves out to the largest circle within  $5M$  of evolution while the gauge adjusts itself near the black hole, slowly shrinks toward the center, until eventually (long dashed lines) it drifts out of shape before the run fails around  $145M$ . (Bruegmann, Tichy, Jansen, gr-qc/0312112).

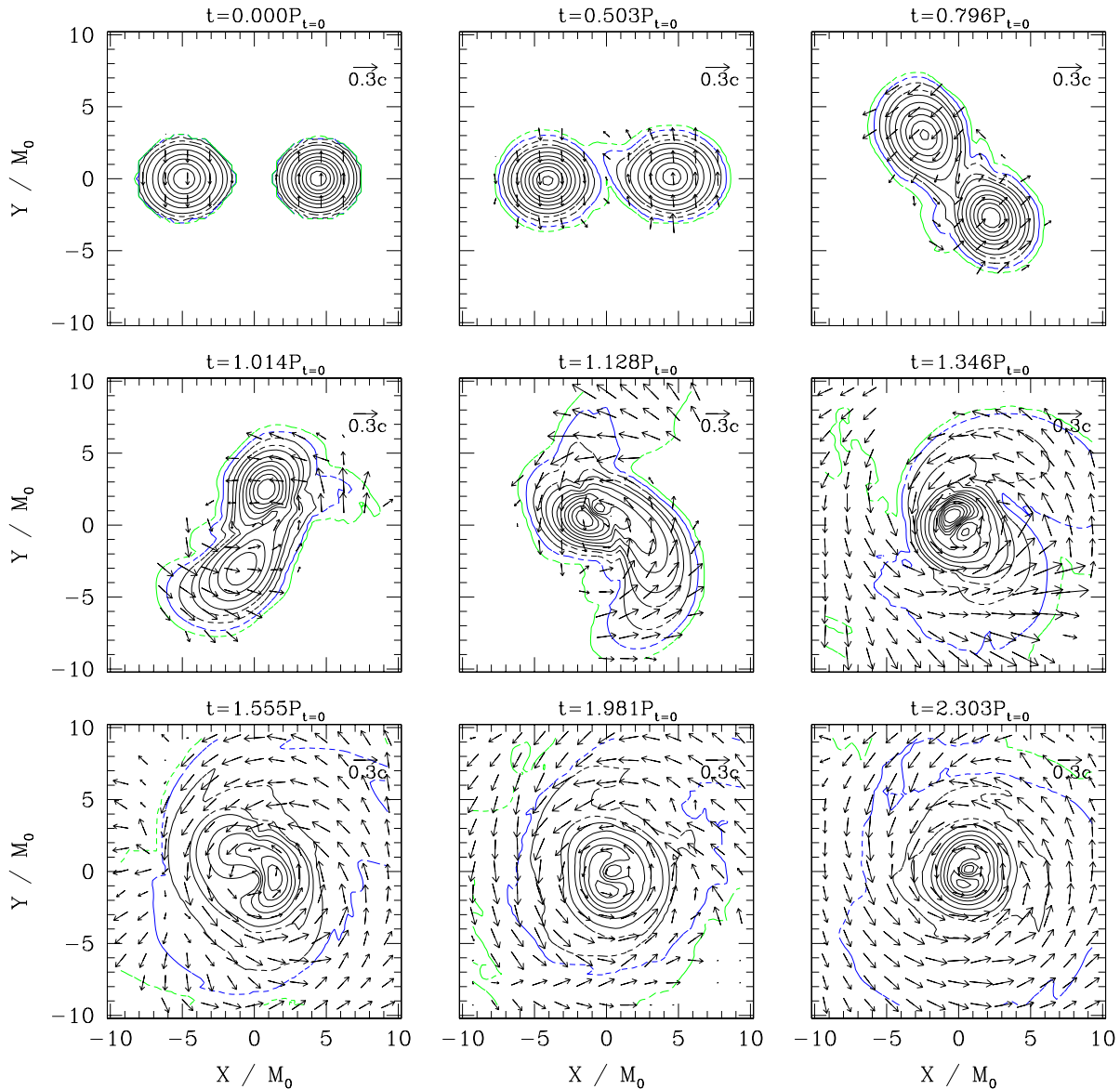


FIG. 1. Snapshots of the density contour curves for  $\rho$  in the equatorial plane for model M1315. The solid contour curves are drawn for  $\rho/0.15 = 1 - 0.1j$  for  $j = 0, 1, 2, \dots, 9$ , and the dashed-solid curves are for  $\rho/0.15 = 0.05, 0.01, 10^{-3}$  and  $10^{-4}$ . Vectors indicate the local velocity field  $(v^x, v^y)$ , and the scale is shown in the upper right-hand corner.  $P_{t=0}$  denotes the orbital period of the quasiequilibrium configuration given at  $t = 0$ . The length scale is shown in units of  $GM_0/c^2$ , where  $M_0$  is the gravitational mass computed at  $t = 0$ . (Shibata, Taniguchi, Uryu, gr-qc/0310030.)

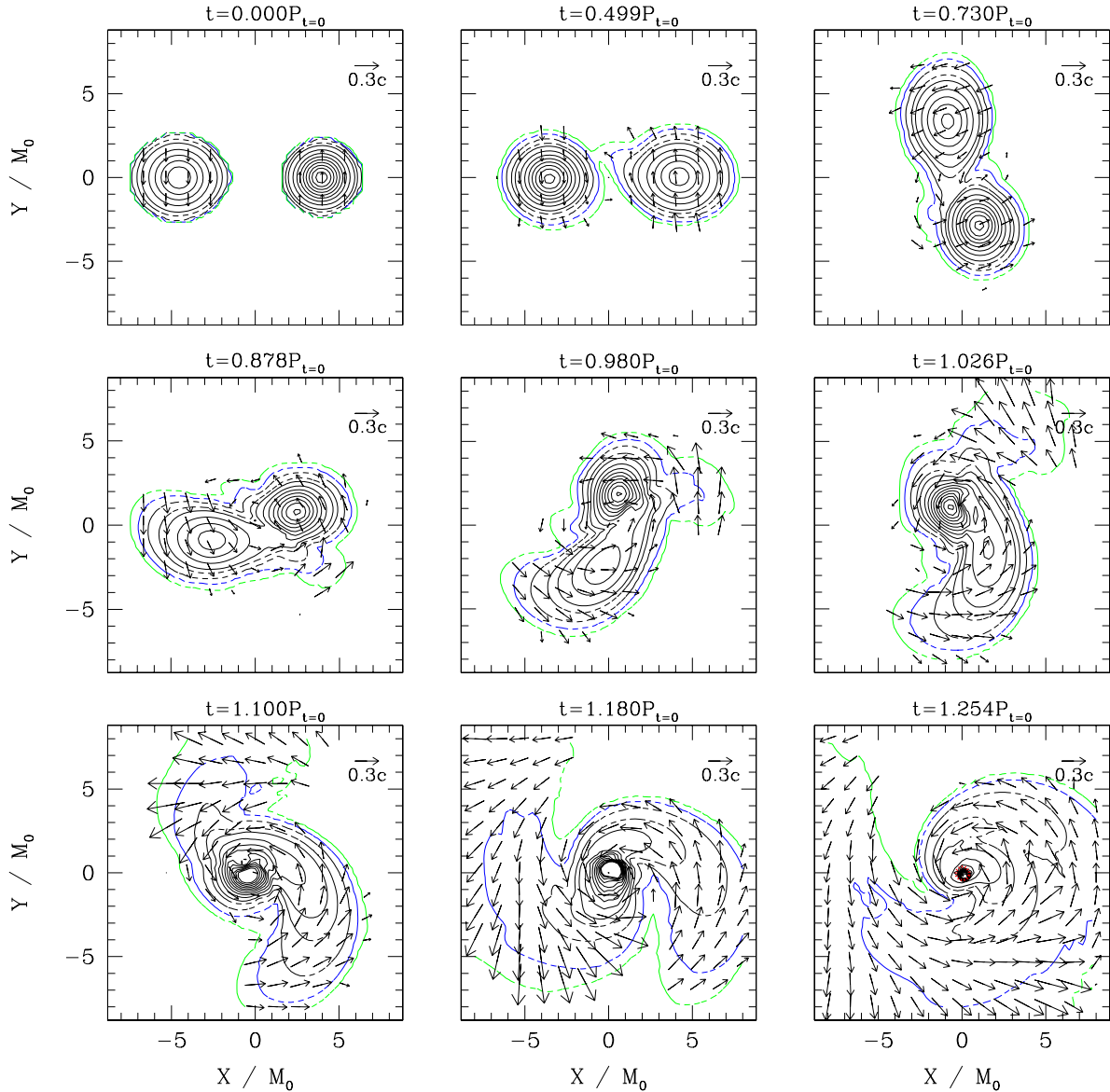


FIG. 2. The same as Fig. 1 but for model M1418. Here, the solid contour curves are drawn for  $\rho/0.20 = 1 - 0.1j$  for  $j = 0, 1, 2, \dots, 9$ , and the dashed-solid curves are for  $\rho/0.20 = 0.05, 0.01, 10^{-3}$  and  $10^{-4}$ . The thick dotted circle in the last panel of radius  $r \sim 0.5M_0$  denotes the location of the apparent horizon. (Shibata, Taniguchi, Uryu, gr-qc/0310030.)



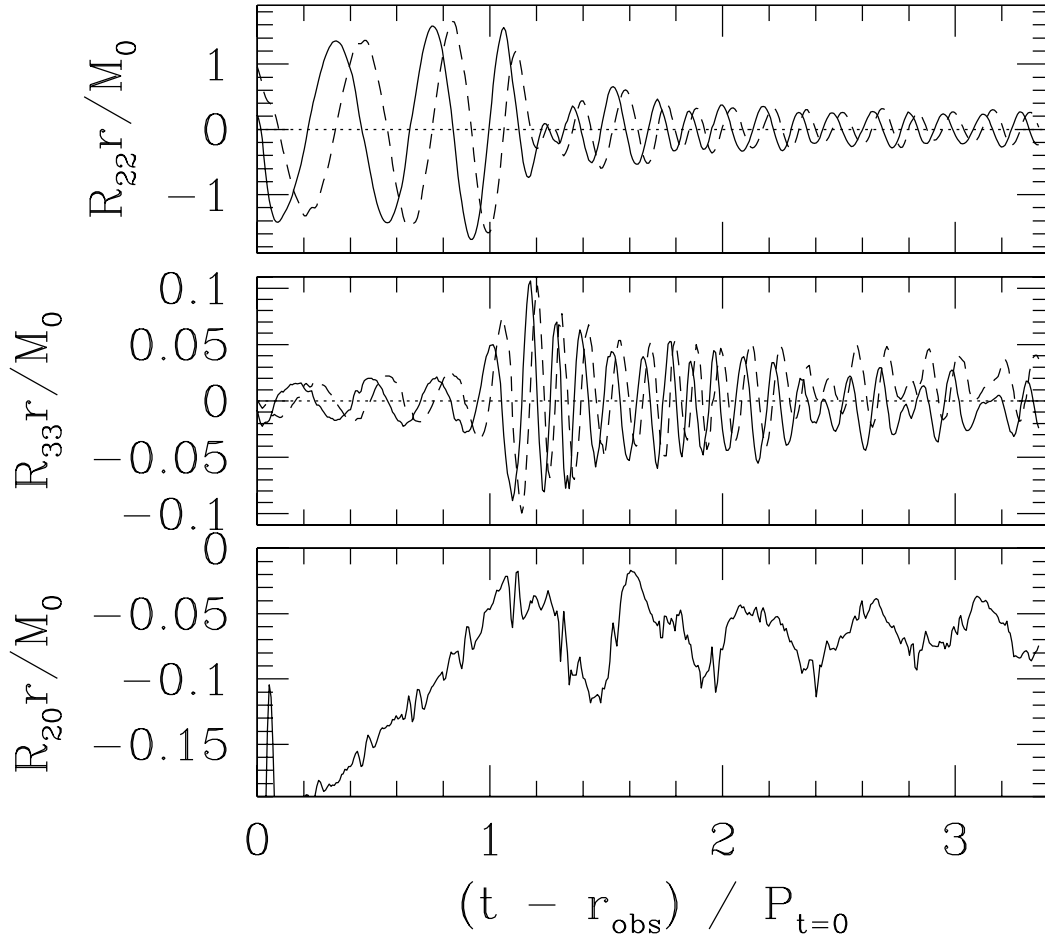


FIG. 3.  $R_{22\pm r}$ ,  $R_{33\pm r}$ , and  $R_{20r}$  as a function of the retarded time for model M1315. The solid and dashed curves for  $R_{22}$  and  $R_{33}$  denote  $R_{lm+}$  and  $R_{lm-}$ . (Shibata, Taniguchi, Uryu, gr-qc/0310030.)

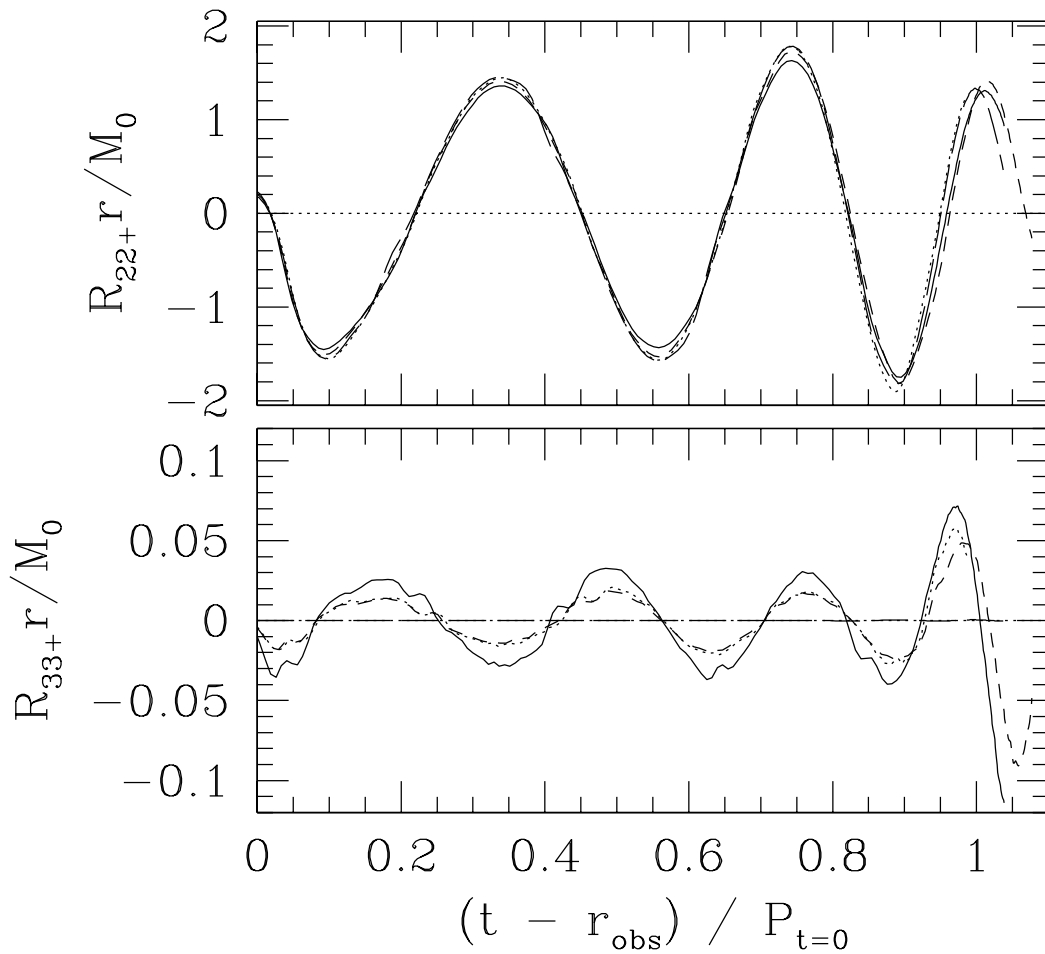
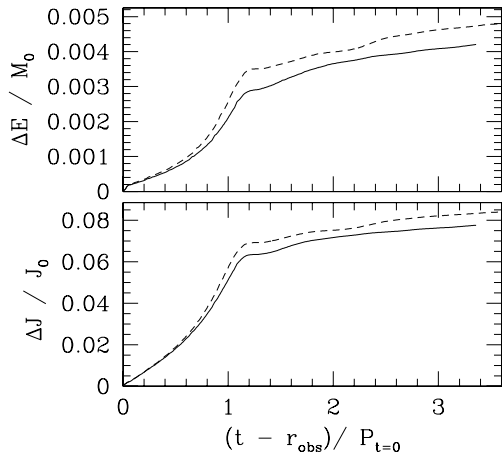
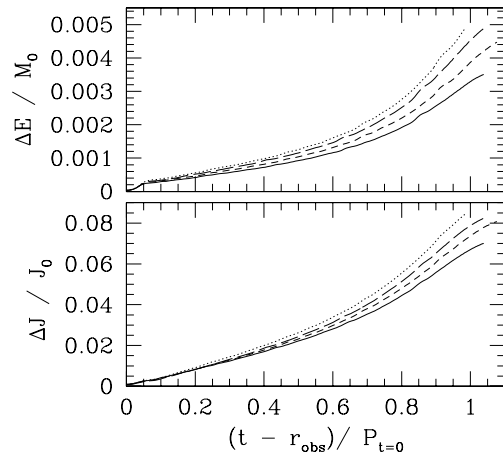


FIG. 4.  $R_{22+r}$  and  $R_{33+r}$  as a function of the retarded time for models M1616 (long-dashed curves), M1517 (dashed curves), M1418 (solid curves), and M159183 (dotted curves). (Shibata, Taniguchi, Uryu, gr-qc/0310030.)



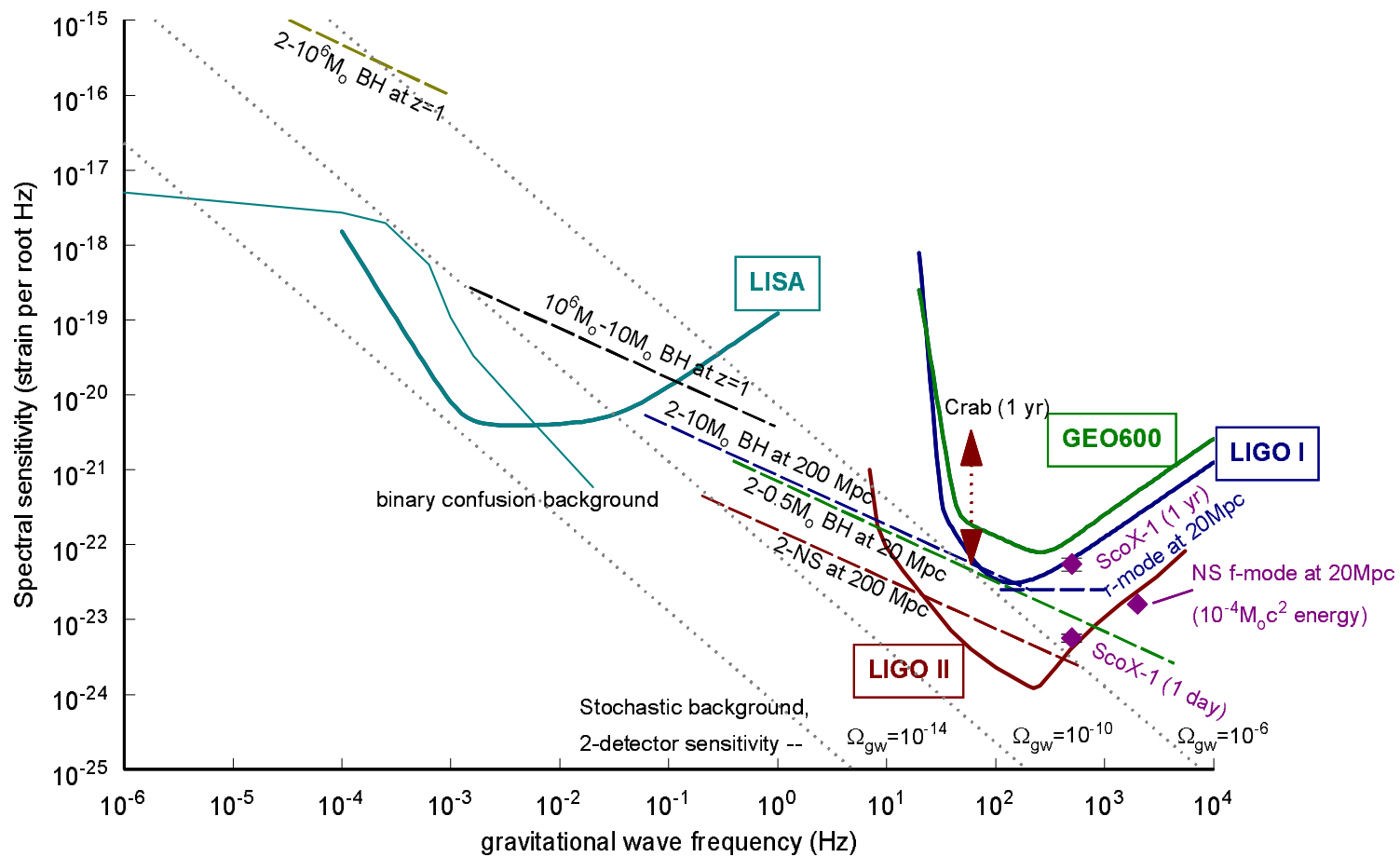
(a)



(b)

FIG. 5. The accumulated energy and angular momentum loss by gravitational radiation as a function of the retarded time (a) for models M1315 (solid curves) and M1414 (dashed curves), and (b) for models M1418 (solid curves), M1517 (dashed curves), M1616 (long-dashed curves), and M159183 (dotted curves). (Shibata, Taniguchi, Uryu, gr-qc/0310030.)

### Sensitivity of Gravitational Wave Interferometers



[Schutz, CQG 16, A131 (1999)]